ELSEVIER

Biophysical Chemistry 60 (1996) 17–27

Biophysical Chemistry

Chlorophyll *a* self-organization in microheterogeneous surfactant systems

A. Agostiano [a,*], L. Catucci [a], G. Colafemmina [a], M. Della Monica [a,b]

[a] *Dipartimento di Chimica, Università di Bari, via Orabona, 4, I-70126 Bari, Italy*
[b] *Centro Studi Chimico-Fisici sull'Interazione Luce-Materia (CFILM), c/o Dipartimento di Chimica, Università di Bari, via Orabona, 4, I-70126 Bari, Italy*

Received 2 October 1995; revised 1 December 1995; accepted 8 December 1995

Abstract

Study on the factors affecting the chlorophyll *a* (Chl *a*) organization with neutral, positively and negatively charged surfactants has been performed by using UV–Vis absorption spectroscopy and circular dichroism. NMR techniques have been employed to investigate the role played in the surfactant reorganization by the state of aggregation of the Chl *a* host. Micelles and lamellar phases have been used during the investigation, carried out at different surfactant and pigment concentrations. Ionic surfactants in micellar phases always promote the Chl *a* aggregation. By varying the non-ionic surfactant concentration, it is possible to modulate the amounts of the aggregated and monomeric forms of Chl *a*. The pigment accelerates the lamellar phase formation and influences the phase organization only above a surfactant concentration of 30%.

Keywords: Chlorophyll *a*; Micellar systems; Self-organization; Surfactants; AOT lamellar phase; Nuclear magnetic resonance spectrometry; UV–Vis spectroscopy

1. Introduction

Chlorophyll *a* (Chl *a*) is the main pigment in the photosynthetic processes of higher plants and algae. The different roles played by this molecule, which is able to act as energy collector in the antenna systems and as primary electron carrier in the photoreactive centers, is mainly due to its molecular organization [1,2]. The absorption spectrum of Chl *a* in vivo is red shifted compared to a solution of pure Chl *a* in a polar solvent [3–5].

Interactions between the chromophores in their aggregated states is believed to be responsible for the shift of the long-wavelength transitions in vivo [3,6], although the stereospecific interactions involving the Mg atom and the C=O groups of the Chl *a* with water or side chains of the amino acids of the environmental proteins have been invoked to explain the effect [7,8]. The charge of the amino acids on the protein network seems also to play a relevant role [9,10].

Recent studies suggest the possibility that the self-organization of the pigment is an inherent property of the chromophores that can affect the polypeptide incorporation into the lipid membrane and, con-

---

[*] Corresponding author.

Elsevier Science B.V.
PII S0301-4622(96)00003-8

sequently, the formation of the protein assembly [11,12].

In the study on factors affecting the Chl *a* organization, microheterogeneous systems formed by surfactants in an aqueous solvent offer the possibility of a hydrophobic microenvironment in which the Chl *a* can be incorporated, thus providing a model of the lipid matrix in which the protein–pigment complexes are located in vivo. In addition, the employment of different surfactants can allow an investigation on the effect of the polar head charge variation on the spectral characteristics of Chl *a*.

In this paper the self-assembly of Chl *a* with neutral, positively and negatively charged surfactants has been investigated by absorption and circular dichroism spectroscopy. In addition, NMR spectroscopy has been employed to investigate the role played in the surfactant reorganization by the aggregation state of the Chl *a* host. Micelles and lamellar phases have been used during the investigation carried out at different surfactant and pigment concentrations.

2. Experimental

2.1. Materials

AOT [sodium bis(2-ethylhexyl)sulfosuccinate) from Sigma was purified according to the procedure recommended by Kunieda and Shinoda. CTAB (hexadecyltrimethylammonium bromide) purchased from Fluka was twice purified with ethanol. Triton X-100 [*p*-(1,1,3,3-tetramethylbutyl)phenoxypoly(oxyethylene)glycol] was obtained from Sigma and used without further purification. ^2H_2O (99.9% ^2H) was from Aldrich.

Chl *a* was isolated from fresh spinach leaves as previously described [13–15] and stored, in the dark, in *n*-pentane at 243 K under an N_2 atmosphere. Purity and concentration were routinely checked using the criteria described elsewhere [16,17].

Appropriate amounts of freshly prepared stock solution were evaporated to dryness. The pigment was then redissolved in detergent solution.

Micellar solutions were prepared by weighing. Lamellar phases were prepared by weighing appropriate amounts of AOT and ^2H_2O into glass tubes which were sealed off immediately. The contents of the tubes was mixed by repeated centrifugation and kept at room temperature. Lamellar phases with Chl *a* were prepared by dissolution of the pigment in a 1% AOT solution and further addition of the proper amount of AOT.

2.2. Methods

Visible absorption spectra were recorded in the 350–800 nm interval with a Cary 3 UV–Vis spectrophotometer (Varian). Circular dichroism (CD) spectra were measured in the 300–800 nm interval, on a JASCO J600 spectropolarimeter (Japan) under N_2 atmosphere. All CD data are reported as elipticity.

Self-diffusion coefficients of CTAB and Triton X-100 were determined using FT-PGSE on a Tesla BS 587 A 80 MHz NMR spectrometer equipped with a pulsed-field gradient unity Stelar and controlled by using HROCH software. The experiments were carried out with a Stejskal–Tanner sequence [18], using a 90°-τ-180°-τ echo with two rectangular field gradient pulses of 0.04 T m^{-1}, separation time $\Delta = 0.1$ s for CTAB and 0.14 s for Triton X-100 and duration time δ. The echo amplitude at 2τ is given by

$$A(2\tau) = A(0)\exp\left[-\gamma^2 G^2 D \delta^2 (\Delta - \delta/3)\right] \qquad (1)$$

were γ is the gyromagnetic ratio, D is the self-diffusion coefficient and time δ was changed from 0.001 to 0.06 ms. Echo amplitudes were analyzed with a non-linear best fit. The temperature of the sample was maintained at 306 ± 0.3 K for CTAB and at 298 ± 0.3 K for Triton X-100 with the variable temperature controller of the spectrometer.

Quadrupolar splittings were obtained by a Varian XL 200, equipped with a superconducting magnet of 4.7 T, with a quadrupolar echo sequence [19].

3. Results and discussion

3.1. Micellar systems

3.1.1. Non-ionic surfactant

The absorption spectra of Chl *a* in Triton X-100 micelles, given in Fig. 1, are recorded at different values of surfactant concentration. The spectra clearly evidence, according to the previously reported data [12,13], the presence of the monomeric form of Chl *a*, with a maximum in the red at 668 nm, and of a long-wavelength form of the pigment with a maximum at 745 nm. The last mentioned absorption band is indicative of the formation of hydrated Chl *a* aggregated forms [3]. The aggregate's structure has been described [14–16] as planar sheet-like, in which two molecules of water are involved in the bridge connecting two Chl *a* molecules.

From the figure it is interesting to note that the amount of aggregated form of the pigment increases with a decreasing surfactant concentration. When the Triton X-100 concentration is lower than 5×10^{-3} M, the aggregate is the prevalent species in solution. At higher surfactant concentrations, the Chl *a* aggregated form is gradually converted, in time, to the monomeric form. This phenomenon is highlighted in the inset of Fig. 1, in which is reported the ratio between the absorbance at 745 and 668 nm, recorded 75 min after sample preparation, as a function of the Triton X-100 concentration. It is evident from Fig. 1 that the ratio between the two species is practically the same for Triton X-100 concentrations lower than 5×10^{-3} M. This ratio decreases with increasing surfactant concentration up to a complete absence of the peak at 745 nm for concentrations exceeding 1×10^{-2} M. In the last mentioned solution the presence of smaller aggregates, as dimers, has been ruled out by the CD data reported in the lower part of Fig. 2. The presence of a non-conservative peak, of negligible intensity, at the wavelength corresponding to the monomer absorption, indicates that this unique Chl *a* species is present in solution. The CD spectrum of the solution at the lowest surfactant concentration, on the contrary, clearly shows the presence of a strong coupling between the dipole

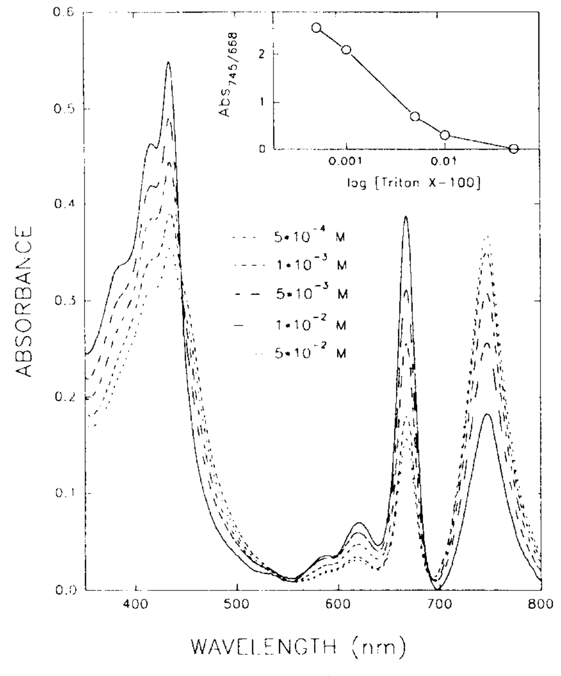

Fig. 1. Absorption spectra of 1×10^{-5} M chlorophyll *a* in Triton X-100 solutions at different surfactant concentrations. Inset: dependence of the ratio between the absorption at 745 nm and the absorption at 668 nm on Triton X-100 concentration.

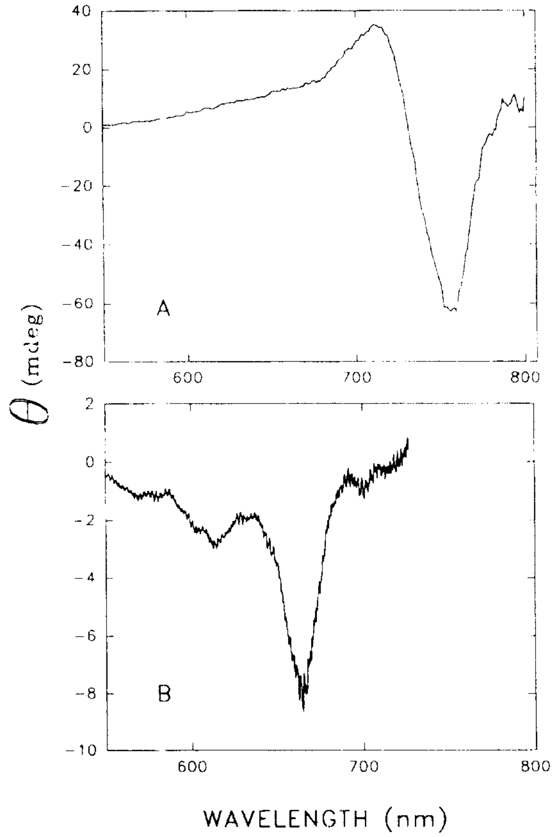

Fig. 2. Circular dichroism spectra of 1×10^{-5} M chlorophyll *a* in (A) a solution of 1×10^{-3} M Triton X-100 and in (B) a solution of 5×10^{-2} M Triton X-100. The measurements were performed with 1 mm and 1 cm path length cells, respectively.

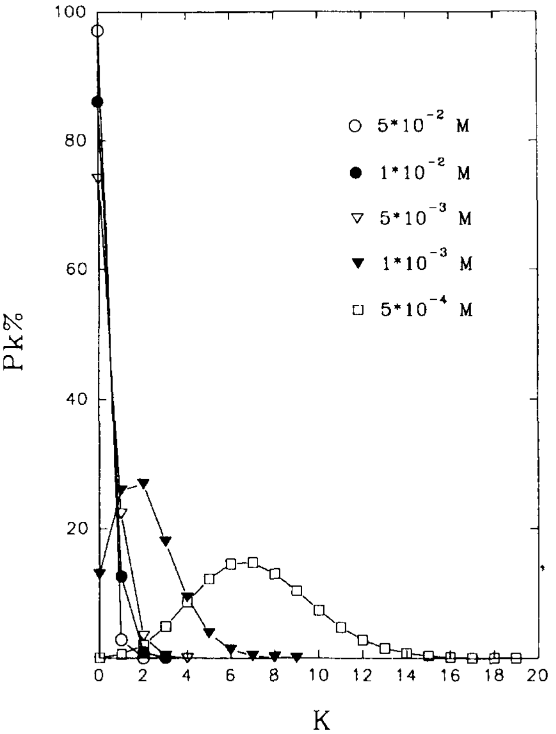

Fig. 3. Poisson distribution of 1×10^{-5} M chlorophyll *a* in micellar solutions at different concentrations of Triton X-100.

transition of different molecules of an aggregate [17,20], as already reported for Chl *a* in wet organic solvents [21]. The non-symmetrical splitting of the two bands and their enlargement seems to indicate the presence of a non-uniform distribution of the different Chl *a* aggregates in the micelles. This is further supported by the Poisson distribution [22] of Chl *a* into the micelles, reported in Fig. 3. The probability that a certain number of *K* Chl *a* molecules is hosted in a micelle, has been evaluated by the following relationship:

$$P_K = Q^K e^{-Q}/K! \qquad (2)$$

where *Q* represents the ratio between the concentration of Chl *a* and of the micelles. The micellar concentration has been calculated considering the amount of free surfactant equal to the critical micellar concentration (CMC), which, for Triton X-100, is 0.24 mM, and assuming an aggregation number of 143 [23]. At higher surfactant concentrations, a relevant part (97%) of the micelles is empty and only a small number of micelles contains two molecules of the pigment. With decreasing surfactant concentration, the number of micelles containing more than two molecules of Chl *a* becomes more and more relevant. A number of molecules of Chl *a* ranging from 2 to 12 is hosted in the largest part of the micelles when the concentration of the surfactant reaches 5×10^{-4} M. The distribution reported in Fig. 3 accounts for the increasing amount of Chl *a* in aggregated form with decreasing Triton X-100 concentration, evidenced by the UV–Vis data of Fig. 1. The presence of large amounts of empty micelles at higher surfactant concentration justifies, in addition, the high rate of polymer dissolution recorded in this solution.

To investigate the role played by Chl *a* aggregation in the reorganization of surfactant molecules into micelles, a structural investigation by self-diffusion NMR has been carried out.

It is well known that the mobility of a system component is greatly influenced by its aggregation state. The analysis of the self-diffusion coefficients can, therefore, be a powerful tool to evaluate the effect of the presence of a host on the microstructure of the system under examination.

In an isotropic system without thermal or concentration gradients, the mean-square displacement of the molecule (or aggregate) in time *t* is given by:

$$\langle r^2 \rangle = 6Dt \qquad (3)$$

Typical self-diffusion coefficients range from 10^{-9} to 10^{-12} m^2 s^{-1}, thus measurements made in an observation period of $\Delta = 0.1$ s, allow to detect mean-square displacements on the order of 0.3–3 μm. The observed self-diffusion coefficient of a distinct component can be expressed as the sum of two terms, according to the two-site model [24]

$$D_{\text{obs}} = p_{\text{free}} D_{\text{free}} + p_{\text{mic}} D_{\text{mic}} \qquad (4)$$

where p_{mic} and p_{free} are the surfactant molar fractions in the micelle and in the monomeric state, respectively. It is evident that D_{mic} can be identified with D_{obs} at high surfactant concentrations characterized by a low CMC value. This D_{mic} value should be corrected for the obstruction effect exerted by the surfactant aggregates on their reciprocal diffusion path. The micellar diffusion coefficient results decreased according to following equation:

$$D_{\mathrm{mic}} = D^{\circ}_{\mathrm{mic}}(1 - k\Phi) \quad (5)$$

where Φ is the volume fraction of surfactant and k is a function of the molecular interactions [25].

Table 1 reports the self-diffusion coefficients for Triton X-100 in ^2H_2O with and without Chl *a*. The data in the absence of Chl *a* show that increasing the surfactant concentration results in a sensible decrease in the Triton X-100 diffusion coefficient, as expected considering that at lower concentration the value of the coefficients is prevalently influenced by the free monomer contribution. Because of the low CMC of Triton X-100 (0.24 mM), the diffusion coefficient relative to the more concentrated solution can be assumed equal to that of the micelle. The extrapolation of the values of the diffusion coefficient at zero concentration removes the error related to the presence of the obstruction factor, giving a value of $D^{\circ}_{\mathrm{mic}} = 5.3 \times 10^{-11}$ m^2 s^{-1}.

Table 1
Measured self-diffusion coefficients of Triton X-100 in ^2H_2O solutions at 25°C without and with 1×10^{-5} M chlorophyll *a*

[Triton X-100] (M)	$D \times 10^{11}$ (m^{2}s^{-1}) no Chl *a*	$D \times 10^{11}$ (m^{2}s^{-1}) Chl *a*
1×10^{-1}	3.0	–
5×10^{-2}	3.6	2.7
1×10^{-2}	4.8	4.5
5×10^{-3}	10.1	6.7
1×10^{-3}	15.9	11.1
1×10^{-4}	23.8	–

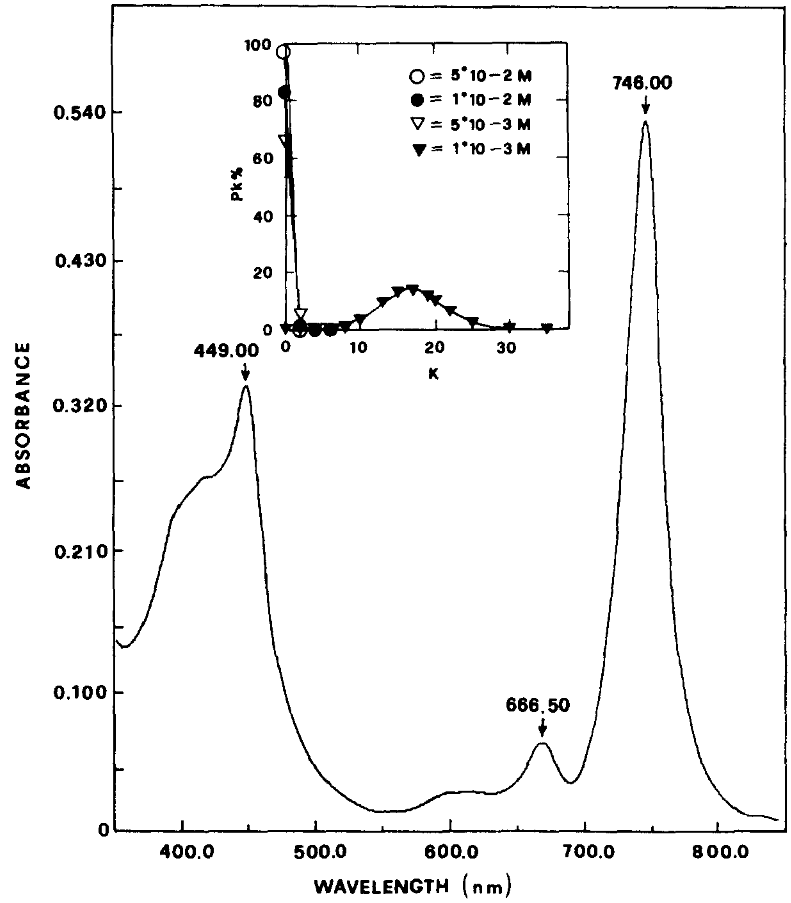

Fig. 4. Absorption spectrum of 1×10^{-5} M chlorophyll *a* in 1×10^{-3} M CTAB solution. Inset: poisson distribution of 1×10^{-5} M chlorophyll *a* in micellar solutions at different CTAB concentrations.

Frequently the determination of the diffusion coefficient can give information about the microstructure of the system, thanks to the correlation existing between D_{mic} and the form of the micelles [26]:

$$D_{\mathrm{mic}} = (kT/6\pi\eta b)F(\mathrm{ar}) \qquad (6)$$

where b is the length of the short axis and $F(\mathrm{ar})$ is a function of the axial ratio. From the Stokes–Einstein equation relative to a spherical aggregate, the hydrodynamic radius obtained is 38 Å. This value falls within the interval of the radius reported in the literature [27–31], which ranges from 31 to 49 Å. On the basis of the average molecular weights obtained with different experimental techniques [32,33], Robson and Dennis have hypothesized the existence of either a classical oblate structure or a spherical non-classical structure [23], in which some oxyethylene chain can be included in the hydrophobic core. The radius calculated assuming this spherical structure is 43 Å, close enough to our finding. This allows us to assume a non-classical spherical form for the Triton X-100 micelles over the entire ranges of temperature and composition examined.

The presence of Chl *a* affects the Triton X-100 diffusion coefficient only at the lowest surfactant concentrations. Actually the data shown in Table 1 indicate a lower value of the coefficient in the presence of Chl *a* above a surfactant concentration of 5×10^{-3} M.

The decrease in the surfactant diffusion rate observed in these systems can be interpreted both in view of the Poisson distribution of the chlorophyll in the micelles, reported in Fig. 3, and on the basis of the increasing peak intensity in the absorption spectra of Fig. 1. Both figures indicate that lower surfactant concentrations imply the presence of a large number of Chl *a* molecules in a single micelle, forming aggregates with an absorption maximum at 745 nm. The relatively high number of pigment molecules for a single micelle seems to modify the structure of the micelle itself. This probably causes an increase in the micellar dimensions resulting in the lowering of its mobility evidenced by the decreasing diffusion coefficients.

3.1.2. Cationic surfactant

The spectra of Chl *a* in a cationic surfactant (CTAB) show the presence of an aggregated form with a maximum at 746 nm, whose intensity largely exceeds that of the monomer at 668 nm (see Fig. 4). No evidence of the blue shift of the Qy band reported in a previous paper by Schmidt et al. [34] has been found in the whole range of concentrations examined.

The formation of self-assembled dimers, whose absorption is strongly red-shifted by the positively charged head group of the surfactant, is invoked to justify the long-wavelength transition of the bacteriochlorophyll *a* in CTAB detergent. In this case the oscillator strength of the Qy band resulted to be noticeably reduced with respect to the Soret band [35]. The peak at 746 nm in Fig. 4 shows the same characteristics of an increased oscillator strength of the Qy band as the Soret band already found in Triton X-100. The enhanced intensity of the Qy band and the vicinity of its wavelength maximum to that recorded in Triton, seems to indicate, in the case of Chl *a* in CTAB, the formation of aggregates larger than dimers.

The full width at half height (FWHH) of the peak in CTAB micelles results to be lower (37 nm) than that of the corresponding peak in Triton X-100 (44 nm), indicating a smaller extent of polydispersity in the cationic surfactant. This evidence is not confirmed by the Poisson distribution of the Chl *a* molecules in the micelles, reported in the inset of Fig. 4. From this distribution a number of Chl *a* for micelles ranging between 10 and 26 is expected. The same distribution (see Fig. 4) shows a reverse dependence of the polymer amount on the surfactant concentration. The data reported in Fig. 5 evidence, on the contrary, that the aggregated form of Chl *a* is always the predominant species in solution at all CTAB concentrations examined, and only a small increase in its amount is found to increase the surfactant concentration. The inadequacy of the Poisson distribution to explain the spectroscopic data arises probably from the fact that the model does not take in account the electrostatic interactions between the charge of the surfactant and the Chl *a* molecule. This interaction can besides account for the small increase in polymer formation with increasing surfactant concentration. The formation of the Chl *a* aggregate can be ascribed to the increased ionic strength and dielectric constant of the solution, as previously reported for Chl *a* in the water-rich region of water–acetonitrile mixtures [16].

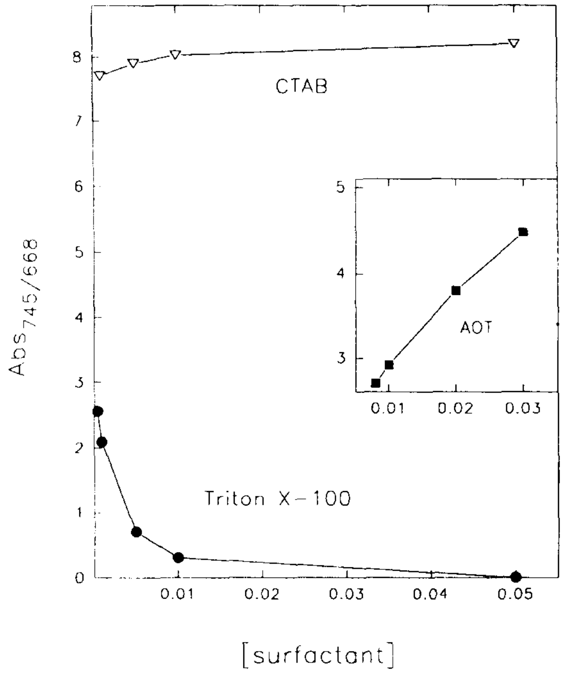

Fig. 5. Dependence of the ratio between chlorophyll *a* absorption at 745 nm and at 668 nm on surfactant concentration. [Chl *a*] = 1×10^{-5} M in all micellar systems reported.

In Table 2 are reported the self-diffusion coefficients relative to the system CTAB–^2H_2O in the presence and absence of Chl *a* at 306 K. The choice of the temperature comes from the consideration that the Krafft point of the surfactant is higher than 298 K [36].

The data obtained in the absence of Chl *a* are in excellent agreement with those already obtained by Lindman. From the extrapolation of the diffusion coefficients in the range 0.05–0.01 M a value of D°_{mic} equal to 7.3×10^{-11} m^2 s^{-1} is obtained. In the reported concentration range this diffusion coefficient corresponds to the micelle's one, as well documented in the literature [36,37].

Table 2
Measured self-diffusion coefficients of CTAB in ^2H_2O solutions at 33°C without and with 1×10^{-5} M chlorophyll *a*

[CTAB] (M)	$D \times 10^{11}$ (m^2 s^{-1}) no Chl *a*	$D \times 10^{11}$ (m^2 s^{-1}) Chl *a*
1×10^{-1}	5.1	5.0
5×10^{-2}	6.5	7.4
1×10^{-2}	9.6	9.5
5×10^{-3}	13.6	14.5
1×10^{-3}	39.0	37.0
5×10^{-4}	59.0	–

Assuming a spherical form for the micelles, from the Stokes–Einstein relation we obtain a hydrodynamic radius equal to 33 Å. Based on geometrical considerations, the hydrodynamic volume is given by:

$$V_h = n(V_s + n_{H_2O} V_{H_2O}) \qquad (7)$$

where n is the aggregation number, V_s the surfactant molecular volume, V_{H_2O} the water molecular volume and n_{H_2O} the number of water molecules per molecule of surfactant.

If we take V_{H_2O} equal to 30 Å^3, n_{H_2O} equal to 10 [32] and V_s equal to 600 Å [38], it is possible to calculate an aggregation number of 167 molecules of surfactant per micelle, a value very close to that reported by Lindman [36].

From Table 2 it is possible to note that the self-diffusion coefficients are influenced only to a minor degree by the presence of Chl *a*. It seems, therefore, reasonable to assume that the presence of the pigment does not modify the micellar structure, as expected from the consideration reported above.

3.1.3. Anionic surfactant

In the inset of Fig. 5 are reported the absorption ratios between the aggregated and the monomeric forms of Chl *a* as a function of the AOT concentration. A small increase in the polymeric species with increasing surfactant concentration is observed, as already observed in CTAB micelles, and, consequently, we do not consider a more detailed investigation of this system fruitful.

From a comparative examination of the data reported in Fig. 5 we can conclude that:

(1) by varying the non-ionic surfactant concentration it is possible to modulate the presence of aggregated and monomeric forms of Chl *a* in solution;

(2) the presence of a charge on the surfactant polar head promotes Chl *a* aggregation;

(3) the Chl *a* aggregated forms in micelles show spectroscopic characteristics similar to those of the Chl *a* aggregates in water–organic solvent mixtures.

3.2. Lamellar system

An extreme case of the microheterogeneous biomodel systems is represented by the lamellar phase that, moreover, exhibits the closest similarity with biological membranes.

Studies on the lamellar formation in the presence of the Chl *a* pigment are, therefore, of great interest for a better understanding of the influence exerted by a host on the lamellar formation and of the role played by the lipid organization in Chl *a* aggregation.

AOT was chosen because of the large lamellar region present in the phase diagram of the AOT–water system [39–41].

The substitution of water with ^2H_2O causes splitting of the NMR signal, due to the interaction of the quadrupole moment of the deuterium nuclei with the electric field gradients such as those existing on the surface of ionic surfactant aggregates. The quadrupole splitting is, consequently, very sensitive to the anisotropy and orientation of the aggregate director axis which undergoes motions which are slow compared with the nuclear relaxation. The value of the quadrupole splitting is given by the equation [42]

$$\Delta\nu = \left[3\chi/(4I(2I-1))\right] \times (3\cos^2\theta - 1 + \eta\sin^2\theta cos 2\phi) \qquad (8)$$

where χ is the coupling constant, θ and ϕ are the orientation of the z-axis of the molecular frame with respect to the liquid crystalline aggregate director, and η represents the asymmetry parameter.

In Table 3 are reported the quadrupole splittings of deuterium relative to lamellar phase of the AOT–^2H_2O system in the presence and in the absence of Chl *a*, at different times after sample preparation. The surfactant concentration covered the range between 14 and 39 wt.%. The measurements were carried out at two different Chl *a* concentrations.

The sample with a AOT concentration of 14% does not evidence any splitting in time, even if the signal enlargement could indicate a slow formation of liquid crystalline phase. The addition of Chl *a* does not imply any change in the spectra.

Increasing the AOT concentration in the range 20–30%, immediately after the preparation of the sample, a unique peak is recorded, whose amplitude increases with increasing surfactant concentration. The lack of quadrupole splitting, in an optically anisotropic phase, can be attributed to biaxial powder aggregates, indicative of the presence of defective structures [43–50].

Table 3
^2H NMR quadrupolar splitting of AOT–^2H_2O lamellar phase, without and with added chlorophyll *a*

[AOT] (wt%) [a]	$\Delta\nu$ (Hz)				
	0 days	15 days	30 days	45 days	660 days[a]
14%	[a]	[a]	[a]	[a]	
A	[a]	[a]	[a]	[a]	[a]
B	[a]	[a]	[a]	[a]	[a]
20%			[a]	[a]	253
A			154	172	221
B			168	205	254
25%	[a]	[a]	309	310	343
A	[a]	322	324	350	346
B	164	325	332	363	
30%	250	312	367	390	443
A	298	382	425	443	434
B	358	450	443	457	458
39%	512			709	652
A	914			867	923
B	1050			832	

[a] Isotropic solution, no quadrupolar splitting.

[b] A = 2×10^{-5} M; B = 5×10^{-5} M as function of the time after sample preparation.

Finally, it is possible to visualize the quadrupole splitting, and the resulting spectra are given by the convolution of two components, one being the previously described two-dimensional powder, the second a spherical uniaxal powder pattern.

These data are completely in agreement with those already reported in the literature for the same system, and have been explained in terms of coexistence with regular lamellae, of curved barriers [48,49], or rippled structures, or interlamellar bilayer disks [47]. An increase in the surfactant concentration results in an increase in the lamellar formation rate. The splitting value recorded after 22 months can be assumed as the equilibrium value for relaxed samples. The ratio between the quadrupole splitting recorded in relaxed and unrelaxed samples [47]:

$$\frac{\Delta\nu^{u}}{\Delta\nu^{r}} = f = \frac{1}{1+\eta} \qquad (9)$$

can be immediately related to the asymmetry parameter η, which assumes the value of zero for a highly ordered lamellar formation.

The f value is, therefore, indicative of the amount of defects in the lamellar phase. This parameter is reported in Fig. 6 for a sample containing 30% of AOT at different times. We can note that 15 days after sample preparation the splitting value is only 70% with respect to the relaxed sample. The presence of Chl *a* at a concentration of 2×10^{-5} M speeds up the formation process of the regular lamellae, as indicated by the fact that after 15 days, f assumes a value of 0.87. This effect is even more evident when the Chl *a* concentration is increased to 5×10^{-5} M. In this case, already after 15 days, f reaches unity, denoting that the lamellar formation process has reached completeness.

In the range of 20–30% AOT it seems, therefore, that Chl *a* plays a kinetic role, catalyzing the lamellar formation, without influencing the equilibrium position. In fact, the quadrupole splitting values in the presence and in absence of Chl *a* do not show significant differences after 22 months (Fig. 6).

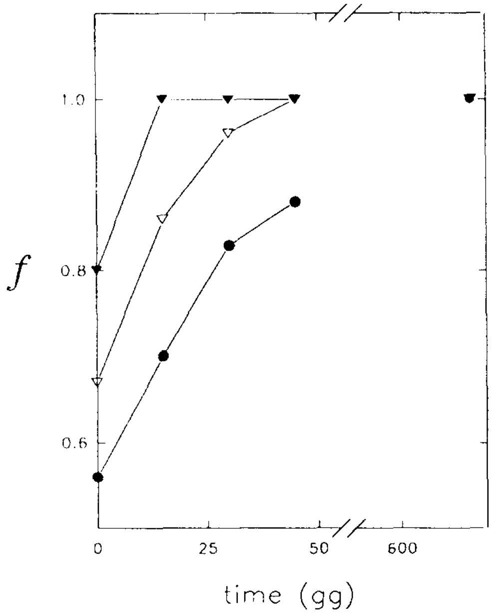

Fig. 6. Time dependence of f parameter in 30% AOT samples (●) in absence and in presence of (▿) 2×10^{-5} M and (▾) 5×10^{-5} M chlorophyll *a*.

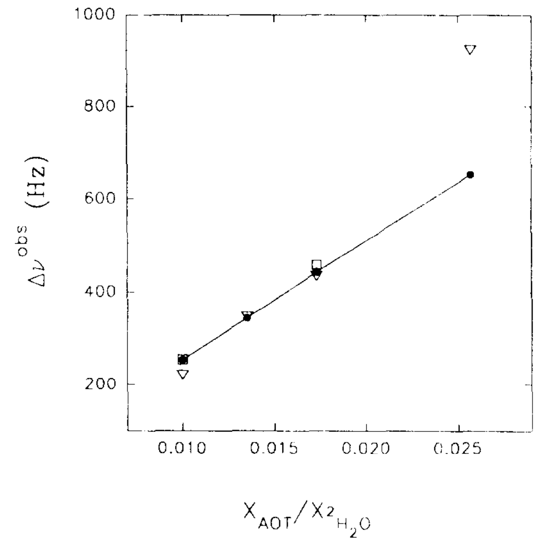

Fig. 7. Observed water deuteron quadrupole splitting for lamellar relaxed samples in AOT–^2H_2O system, (●) in absence and in presence of (▿) 2×10^{-5} M and (□) 5×10^{-5} M chlorophyll *a*, as a function of the molar ratio of surfactant to water.

Further conclusions can be drawn by the evaluation of the order parameter. If we assume a fast ^2H_2O exchange between the water bound to the surfactant molecules and the water free in the bulk [51], and that only the bound water produces the quadrupole splitting, it is possible to obtain the following relationship between the order parameter S and the observed splitting:

$$\Delta\nu_{obs} = 3/4 X_S n(\chi S)_b / X^2_{H_2O} \qquad (10)$$

where X_S and $X^2_{H_2O}$ are surfactant and ^2H_2O molar fraction respectively, n is the average hydration number of the surfactant, taken equal to 2 [51], and χ is the quadrupole splitting constant, equal to 220 kHz for water.

According to this model a plot of $\Delta\nu_{obs}$ against the ratio between the molar fractions of the surfactant and of water, gives a straight line whose slope is equal to $n(\chi S)_b$. A direct proportionality between the molar fraction ratio and the ^2H_2O splitting is indeed observed for relaxed samples without Chl *a* in the whole concentration range under investigation (see Fig. 7). In the presence of Chl *a*, the upper limit of linearity drops to 30%. In the surfactant concentration range of 14–30%, an order parameter of 0.06 is calculated for both samples with and without Chl *a*, ruling out the possibility of an active role of the

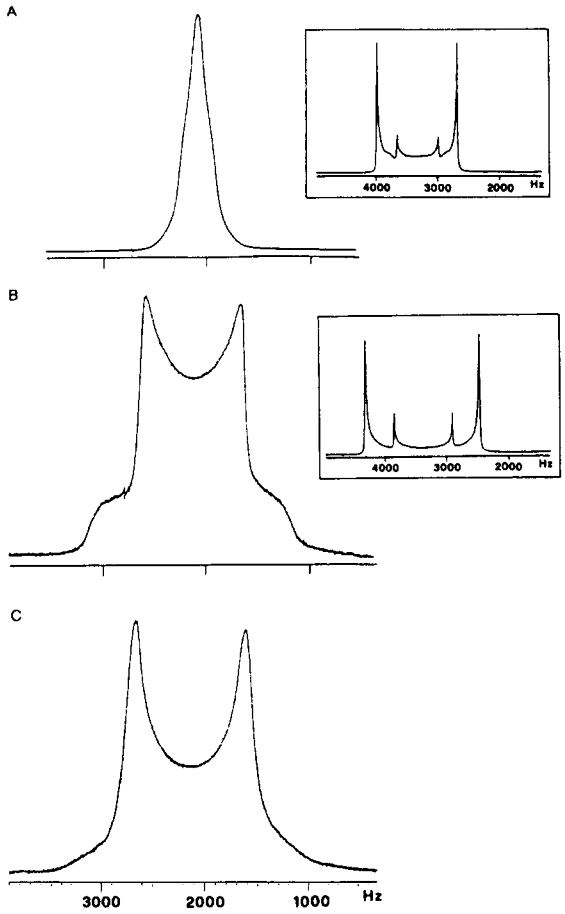

Fig. 8. Deuterium NMR spectra recorded immediately after the preparation of samples containing 39.44% AOT (A) in absence and in presence of (B) 2×10^{-5} M chlorophyll *a* and (C) 5×10^{-5} M chlorophyll *a*. Insets: deuterium NMR spectra of the same samples recorded 22 months after their preparation.

pigment in the equilibrium organization of the surfactant up to 30%.

A rather different situation is observed for samples at higher concentration (39%) of AOT. In Fig. 8 are reported the quadrupole splitting spectra of the samples containing the 39.44% AOT in the absence and presence of Chl *a* at different concentrations. Different from what was observed at the other concentrations examined, immediately after the preparation, the samples containing Chl *a* show a pronounced quadrupole splitting, whose amplitude increases with increasing Chl *a* concentration (see Fig. 8 and Table 3).

Still after 22 months, the splitting observed in samples containing Chl *a* results to be noticeably greater than that in samples containing only AOT. The order parameter of the relaxed samples with pigment is consequently higher than that calculated for the sample without Chl *a*. At this surfactant concentration, Chl *a* seems, consequently, to play a role not only in accelerating the lamellar formation, but also in improving the molecular order.

The spectra at 39.44% AOT show in addition the characteristic of a quadrupole splitting in which the external peaks are more intense than the internal ones (see insets of Fig. 8). This experimental evidence shown by samples with and without Chl *a*, indicates, a preferential orientation of the lamellae with the external magnetic field [42]. An anomalous behavior of the AOT–^2H_2O system at this surfactant concentration has already been evidenced by Fontell with X-ray measurements, and successively attributed to mechanically induced deformation of regular lamellae [52], or, alternatively, to the formation of extra bilayers pockets [47], by means of self-diffusion PFG NMR and conductivity measurements.

It is beyond the aim of this paper to investigate the factors influencing the system organization at this concentration, although further experiments (self-diffusion, relaxation times, conductivity) are in progress in our laboratory to better characterize the role played by Chl *a* in influencing the lamellar order.

The last information relative to this system comes from the UV–Vis spectra of the samples containing Chl *a*. The pigment appears to be always in its aggregated form, with a maximum at 747 nm, in the just prepared samples, characterized by the absence of quadrupole splitting. The final formation of the lamellae results in the desegregation of Chl *a* which, after 30 days, appears in its monomeric state. This seems to indicate that the pigment preferentially occupies the intralamellar space, in the hydrophobic core of the phase.

In conclusion, from the data reported above we can assume that Chl *a* plays a relevant role in accelerating the formation of lamellar structures, without influencing their organization up to a surfactant concentration of 30%. The formation of lamellae, on the contrary, always influences the aggregation state of Chl *a*. Higher surfactant concentration, unexpectedly, shows an active role of Chl *a* in better bilayer organization, evidencing that even very low pigment concentration can influence the hosting phase.

Acknowledgements

We thank Prof. A. Sacco and Prof. A. Ceglie for the opportunity to use the Tesla NMR spectrometer. We also wish to thank Dr. G. Palazzo for CD measurements and for helpful discussions. This work has been supported by CNR–Progetto Finalizzato Chimica Fine II.

References

[1] G. Forti, in J. Amesz (Ed.), New Comprehensive Biochemistry, Vol. 15, Elsevier, Amsterdam, 1987, p. 1.
[2] A.J. Hoff, in F.K. Fong (Ed.), Molecular Biology Biochemistry and Biophysics, Vol. 35, Springer Verlag, Berlin, 1982, p. 80.
[3] J.J. Katz, M. K. Bowman, T.J. Michalski and D.L. Worcester, in H. Scheer (Ed.), Chlorophylls, CRC Press, Boca Raton, FL, 1991, p. 212.
[4] A. Agostiano, K.A. Butcher, M. S. Showell, A.J. Gotch, and F.K. Fong, Chem. Phys. Lett., 137 (1987) 37.
[5] H. Blaha, P. Kis and H. Springer-Lederer, Anal. Biochem., 112 (1981) 282.
[6] A Scherz, V. Rosenbach-Belkin and J.A.E. Fisher, in H. Scheer (Ed.), Chlorophylls, CRC Press, Boca Raton, FL, 1991, p. 237.
[7] L.L. Shipman, J. Phys. Chem., 81 (1977) 2180.
[8] J.R. Norris, H. Scheer, M.E. Druyan and J.J. Katz, Proc. Natl. Acad. Sci. USA, 74 (1977) 4897.
[9] J. Eccles and B. Honig, Proc. Natl. Acad. Sci. USA, 80 (1983) 4959.
[10] R.C. Davis, S.L. Ditson, A.F. Fentiman and R.M. Pearlstein, J. Am. Chem. Soc., 103 (1981) 6823.
[11] J. Gottstein, A. Scherz and H. Scheer, Biochim. Biophys. Acta, 1183 (1993) 413.
[12] A. Scherz, V. Rosenbach-Belkin and J.R.E. Fisher, Proc. Natl. Acad. Sci. USA, 87 (1990) 5430.
[13] J.P. Chauvet, R. Viovy, R. Santus and E.J. Land, J. Phys. Chem., 85 (1981) 3449.
[14] D.L. Worcester, T.J. Michalski and J.J. Katz, Proc. Natl. Acad. Sci. USA, 83 (1986) 306.
[15] H.C. Chow, R. Serlin and C.E. Strouse, J. Am. Chem. Soc., 97 (1975) 7230.
[16] A. Agostiano, M. Della Monica, G. Palazzo and M. Trotta, Biophys. Chem., 47 (1993) 193.
[17] V. Fidler and A.D. Osborne, J. Chem. Soc. Chem. Commun., (1980) 1056.
[18] O. Stejskal and J.E. Tanner, J. Chem. Phys., 52 (1965) 288.
[19] J.H. Davis, Biochim. Biophys. Acta, 737 (1983) 117.
[20] A.G. Volkov, M.I. Gugsehashvili, M.D. Kandelaki, V.S. Markin, B. Zelent, G. Munger and R.M. Leblanc, Photochem. Photoelectrochem. Org. Inorg. Mol. Thin Films, 1436 (1991) 68.
[21] M.D. Kandelaki, A.G. Volkov, V.V. Shubin and L.I. Boguslawsky, Biochim. Biophys. Acta, 893 (1987) 170.
[22] P.P. Infelta and M. Gratzel, J. Chem. Phys., 70 (1979) 179.
[23] R.J. Robson and E.A. Dennis, J. Phys. Chem., 81 (1977) 1075.
[24] P.G. Nilsson, H. Wennerstrom and B. Lindman, J. Am. Chem. Soc., 87 (1983) 1377.
[25] T. Ohtsuki and K. Okano, J. Chem. Phys., 77 (1982) 1443.
[26] P.C. Hiementz, Principles of Colloid and Surface Chemistry, Marcel Dekker, New York, 2nd ed., 1986.
[27] H.H. Paradies, J. Phys. Chem., 84 (1980) 599.
[28] W. Brown, R. Rymden, J. van Stam, M. Almgren and G. Svensk, J. Phys. Chem., 93 (1989) 2512.
[29] A.S. Sadaghiani and A. Khan, Langmuir, 7 (1991) 898.
[30] G.D.J. Phillies, J. Stott and S.Z. Ren, J. Phys. Chem., 97 (1993) 11563.
[31] K. Streletzky and G.D.J. Phillies, Langmuir, 11 (1995) 42.
[32] L.M. Kushner and D. Hubbard, J. Phys. Chem., 58 (1954) 1163.
[33] M. Corti and V. Degiorgio, Opt. Commun., 14 (1975) 358.
[34] A. Schmidt, J. Gottstain, H. Sheer and A. Scherz, Z. Naturforsch., 45C (1990) 729.
[35] J. Gottstein, A. Scherz and H. Scheer, Biochim. Biophys. Acta, 1183 (1993) 413.
[36] B. Lindman, M. C. Puyal, N. Kamenka, R. Rymden and P. Stilbs, J. Phys. Chem., 88 (1984) 5048.
[37] D. Maciejewska, A. Khan and B. Lindman, Prog. Coll. Polym. Sci., 73 (1987) 174.
[38] F. Reiss-Husson and V. Luzzati, J. Phys. Chem., 68 (1964) 3504.
[39] J. Rogers and P.A. Winsor, Nature, 216 (1967) 477.
[40] P.A. Winsor, Chem. Rev., 68 (1980) 1.
[41] P.A. Winsor, Mol. Cryst. Liq. Cryst., 12 (1971) 141.
[42] B.J. Forrest and L.W. Reeves, Chem. Rev., 81 (1981) 1.
[43] K. Fontell, J. Colloid Interface Sci., 44 (1973) 318.
[44] I. Lundstrom and K. Fontell, Chem. Phys. Lipids, 15 (1975) 1.
[45] J. Rogers and P.A. Winsor, J. Colloid Interface Sci., 30 (1969) 247.
[46] R. Faiman, I. Lundstrom and K. Fontell, Chem. Phys. Lipids, 18 (1977) 73.
[47] P.T. Callaghan and O. Soderman, J. Phys. Chem., 87 (1983) 1737.
[48] G. Chidichimo, C. La Mesa, G.A. Ranieri and M. Terenzi, Mol. Cryst. Liq. Cryst., 150B (1987) 221.
[49] G. Chidichimo, D. Imbardelli, A. Golemme and G.A. Ranieri, Mol. Cryst. Liq. Cryst., 201 (1991) 125.
[50] L. Coppola, R. Muzzalupo, G.A. Ranieri and M. Terenzi, Langmuir, 11 (1995) 1116.
[51] N.O. Persson and B. Lindman, J. Phys. Chem., 79 (1975) 1410.
[52] F.D. Blum, E.I. Franses, K.D. Rose, R.G. Bryant and W. G. Miller, Langmuir, 3 (1987) 448.